International Journal of Chemical, Materials and Biomolecular Sciences
ISSN: 2415-6620
Vol:12, No:8, 2018

Non-Linear Load-Deflection Response of Shape Memory Alloys-Reinforced Composite Cylindrical Shells under Uniform Radial Load

Behrang Tavousi Tehrani, Mohammad-Zaman Kabir

***Abstract*—**Shape memory alloys (SMA) are often implemented in smart structures as the active components. Their ability to recover large displacements has been used in many applications, including structural stability/response enhancement and active structural acoustic control. SMA wires or fibers can be embedded with composite cylinders to increase their critical buckling load, improve their load-deflection behavior, and reduce the radial deflections under various thermo-mechanical loadings. This paper presents a semi-analytical investigation on the non-linear load-deflection response of SMA-reinforced composite circular cylindrical shells. The cylinder shells are under uniform external pressure load. Based on first-order shear deformation shell theory (FSDT), the equilibrium equations of the structure are derived. One-dimensional simplified Brinson's model is used for determining the SMA recovery force due to its simplicity and accuracy. Airy stress function and Galerkin technique are used to obtain non-linear load-deflection curves. The results are verified by comparing them with those in the literature. Several parametric studies are conducted in order to investigate the effect of SMA volume fraction, SMA pre-strain value, and SMA activation temperature on the response of the structure. It is shown that suitable usage of SMA wires results in a considerable enhancement in the load-deflection response of the shell due to the generation of the SMA tensile recovery force.

***Keywords*—**Airy stress function, cylindrical shell, Galerkin technique, load-deflection curve, recovery stress, shape memory alloy.

I. Introduction

DUE to their unique characteristics, such as high stiffness-to-weight, high strength-to-weight, and high fatigue resistance, composite materials have gained notable attention in the recent years. Applications of composite materials in more and more sophisticated designs are due to the recent advances in this field. One of the major structural components with a wide range of applications in the structural, mechanical, civil, and aerospace engineering fields is cylindrical panels and shells. When composite cylindrical shells are loaded under thermo-mechanical forces, the buckling phenomenon and large non-linear deflections happen. As a result, the study of load-deflection response of laminated cylindrical shells, introducing an appropriate procedure in order to enhance their response is an important step for design purposes.

SMA fibers or wires can be used to improve the stability of composite structures. Under large deflections (up to 8∼10%), SMAs have the ability to gain their original shape. This ability is the result of the transformation of two solid phases, martensite to austenite. In this process, SMA wires or fibers are heated above the austenite finish temperature. Consequently, the phase transformation produces an enormous amount of tensile recovery stresses under restrained conditions, which can be used to enhance the load-deflection response of SMA composite laminated structures. These types of materials are well-known as smart materials.

Very few studies have been conducted to investigate the effects of SMA wires and fibers on the static and dynamic response of composite thin-walled cylindrical shells or other types of SMA cylindrical shell structures. Some literature survey is as follows.

Paine et al. [1] conducted an investigation of adaptive hybrid composite cylinders utilizing active SMA composite layers for implementing in high-pressure vessel applications. They used an analytical approach in their study and observed that peak tensile hoop stresses and radial expansion of the cylinder inner walls could be substantially reduced. Burgueño et al. [2] carried out a numerical study on the post-buckling response of cylindrical shells under axial compression for application in smart structures. Damanpack et al. [3] studied the axisymmetric thermo-mechanical behavior of Epoxy/ Aluminum matrix composite cylinders reinforced with SMA fibers under internal pressure, axial, torsional, and thermal loading based on the micro-macro method. Nemat-Nasser et al. [4] examined compressive tests on cylindrical shells consisting of Ni-Ti SMA, 7075 aluminum, and maraging steel to study their buckling behavior under quasi-static loading conditions. They reported that the stress-induced martensite formation in Ni-Ti shape memory shells appears to have a profound influence on the shells' unstable deformation, and this can be effectively used to mitigate potential catastrophic failure. A method for solving the problem of the stability of a cylindrical shell made of a SMA was proposed by Sil'chenko et al. [5]. Birman [6] proposed a study on the effects of composite and SMA stiffeners on the stability of composite cylindrical shells subjected to a compressive load. The governing equations were developed based on the Love's first approximation theory and smeared stiffeners technique. It was proven that SMA stiffeners enhanced the upper and lower buckling loads. A semi-analytical solution was presented to

Behrang Tavousi Tehrani is with the Department of Civil and Environmental Engineering, Amirkabir University of Technology, Tehran, Iran (e-mail: behrang.tavousi@aut.ac.ir).

Mohammad-Zaman Kabir is with the Department of Civil and Environmental Engineering, Amirkabir University of Technology, Tehran, Iran (corresponding author, phone: +98 21 64543000; e-mail: mzkabir@aut.ac.ir).

investigate the thermal buckling behavior of SMA hybrid composite laminated shells with cross-ply lay-up by Asadi et al. [7]. They generally concluded that an increase in the SMA fiber volume fraction or SMA fiber pre-strain results in a remarkable enhancement in the critical buckling temperature. In another work, Asadi et al. [8] focused on the enhanced thermal stability of FG-sandwich cylindrical shells by SMA. The results showed that SMA fibers could postpone the onset of thermal bifurcation of FG/SMA/FG sandwich cylinders and had a significant effect on the thermal buckling mode of the structure. Amini and Nemat-Nasser [9] performed a set of numerical simulations to study the dynamic and quasi-static response of thin-walled circular cylindrical shells consisting of SMA. Akbari and Khalili [10] conducted an experimental investigation on the buckling behavior of SMA cylindrical composite shells. Liu and Du [11] performed an analytical solution for pseudo-elastic response of a SMA thick-walled cylinder subjected to external pressure. Li et al. [12] investigated the frequency control of simply supported cylindrical shells with Light-activated Shape Memory Polymers (LaSMP). They reported that LaSMP is a novel and effective actuation mechanism to control the frequency of cylindrical shells. Frouzesh and Jafari [13] presented the radial vibrations of simply supported SMA cylindrical shell under internal pressure using DQM method. They used SMA's pseudo-elastic feature in their work. In a recent work, Salim et al. [14] have used GDQ numerical method in order to determine natural frequencies and buckling temperature of an SMA circular cylindrical shell.

To the best of the authors' knowledge, the lack of analytical investigation on the non-linear load-deflection response of composite cylindrical shell reinforced with SMA wires under radial load encouraged the authors to focus on this subject. The present study uses a semi-analytical approach for load-deflection response of SMA composite cylindrical shell subjected to uniform radial load. Galerkin procedure is carried out to solve the partial differential equation of motion and convert it to an algebraic equation. This formulation is based on FSDT. Some parametric studies such as effects of SMA volume fraction, SMA activation temperatures, and SMA pre-strain value on the response of the structure are presented in this paper.

II. 1-D Brinson's Constitutive for SMA Modeling

A 1-D SMA model is used in this work. It shows a simple constitutive equation to simulate the characteristics of the SMA. In Brinson's model, the total martensite fraction (ξ) is sum of the stress-induced fraction (ξ_s) and the temperature-induced martensite fraction (ξ_T) as:

$$\xi = \xi_s + \xi_T \tag{1}$$

The SMA's Young modulus is assumed to be based on the Reuss definition [15] as:

$$E_s(\xi) = \frac{E_A}{1+\left(\frac{E_A}{E_M}-1\right)\xi} \tag{2}$$

where E_A and E_M are the Young modulus of SMA in austenite phase and martensite phase, respectively. The tensile recovery stress of SMA during phase transformation can be determined by using the simple Brinson's model [16] as:

$$\sigma = E_s(\xi)(\varepsilon - \varepsilon_L\xi_s) + \Theta\Delta T \tag{3}$$

where $\sigma, \varepsilon, \Theta, \Delta T$, and ε_L refer to the stress, strain, thermo-elastic tensor, temperature change, and maximum recoverable strain, respectively. The reference temperature is assumed to be 20 ℃.

Calculation of the phase transformation from martensite to austenite can be written [17] as:

$$\begin{aligned}
&\text{for } T > A_s, C_A(T-A_f) < \sigma < C_A(T-A_s)\\
&\xi = \frac{\xi_0}{2}\left\{cos\left[\frac{\pi}{A_f-A_s}(T-A_s-\frac{\sigma}{C_A})\right]+1\right\}\\
&\xi_s = \xi_{s0} - \frac{\xi_{s0}}{\xi_0}(\xi_0-\xi)\\
&\xi_T = \xi_{T0} - \frac{\xi_{T0}}{\xi_0}(\xi_0-\xi)
\end{aligned} \tag{4}$$

where the subscript "0" denotes for the initial condition of the parameter. The constant C_A shows the relationship between temperature and critical phase transformation stress in Brinson's model. A_s, A_f, and T denote for austenite start temperature, the austenite finish temperature, and temperature, respectively. During phase transformation, the SMA wires are restrained to freely recover their initial strains (SMA wires are embedded in the composite matrix). Consequently, large tensile recovery force is produced and can be used to enhance the load-deflection response of a composite shell. A laminated composite cylindrical shell with length, mean radius and thickness of L, R, and t is considered. Fig. 1 shows a diagram of SMA composite cylindrical shell and its coordinate system.

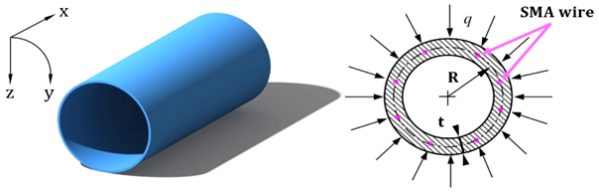

Fig. 1 The configuration of SMA composite cylindrical shell and its coordinate system

Table I provides the SMA material properties.

TABLE I
Thermo-Mechanical Properties of The SMA Material

Material Property	Property value [18].
$(E_A, E_M)\ GPa$	$(67, 23.6)$
(M_s, M_f) ℃	$(18.4, 9)$
(A_s, A_f) ℃	$(34.5, 49)$
$(C_A, C_M)\ MPa℃^{-1}$	$(13.8, 8)$
$(\sigma_{cr}^s, \sigma_{cr}^f)\ MPa$	$(100, 170)$
$\Theta\ MPa℃^{-1}$	0.55
α_s $℃^{-1}$	10.26×10^{-6}
$(\upsilon_s, \varepsilon_L, \xi_{T0})$	$(0.33, 0.067, 0)$

Fig. 2 shows the stress-strain curve of the SMA and experimental data obtained from Liang's work [19] at different temperatures. The results show a good agreement between the Brinson's model and experimental work.

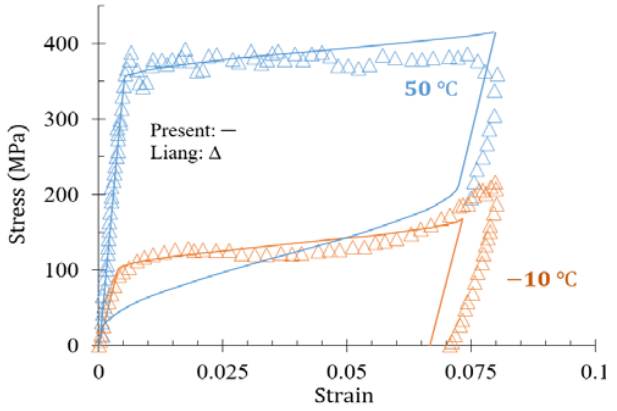

Fig. 2 SMA stress-strain curves

In Fig. 3, the SMA recovery stress based on (3) is obtained for different pre-strain values. Also, the results for pre-strains equal to 1.34%, 1%, and 0.5% are presented as per by Lee et al. [20], Roh et al. [21], and Abdollahi et al. [22].

Fig. 4 shows that, as the pre-strain value increases, the austenite finish temperature also increases, but the austenite start temperate remains constant.

Fig. 5 depicts the temperature-dependent elastic modulus of SMA wire during the phase transformation. The curves have been plotted using (1)-(4) for different SMA pre-strain values. The SMA wires are embedded in the composite matrix.

III. Constitutive Equations

In this work, the effective engineering parameters, E_1, E_2, G_{12}, υ_{12}, α_1, and α_2 are based on the multi-cell micromechanics formulation [23] as:

$$E_1 = E_s(\xi)V_s + E_{1m}(1 - V_s) \tag{5}$$

$$E_2 = E_{2m}\left[\left(1 - \sqrt{V_s}\right) + \frac{\sqrt{V_s}}{1-\sqrt{V_s}\left(1-\frac{E_{2m}}{E_s(\xi)}\right)}\right] \tag{6}$$

$$G_{12} = G_{12m}\left[\left(1 - \sqrt{V_s}\right) + \frac{\sqrt{V_s}}{1-\sqrt{V_s}\left(1-\frac{G_{12m}}{G_s(\xi)}\right)}\right] \tag{7}$$

$$\upsilon_{12} = \upsilon_s V_s + \upsilon_{12m}(1 - V_s) \tag{8}$$

$$\alpha_1 = \frac{E_s(\xi)V_s\alpha_s + E_{1m}(1-V_s)\alpha_{1m}}{E_s(\xi)V_s + E_{1m}(1-V_s)} \tag{9}$$

$$\alpha_2 = \frac{E_{2m}}{E_2}\left[\alpha_{2m}\left(1 - \sqrt{V_s}\right) + \frac{\alpha_{2m}\sqrt{V_s} - V_s(\alpha_{2m} - \alpha_s)}{1-\sqrt{V_s}\left(1-\frac{E_{2m}}{E_s(\xi)}\right)}\right] \tag{10}$$

$$G_s(\xi) = \frac{E_s(\xi)}{2(1+\upsilon_s)} \tag{11}$$

where the "m" and "s" subscripts denote for the composite matrix and SMA wires, respectively. Material parameters, E_1, E_2, G_{12}, υ_{12}, α_1, α_2, $G_s(\xi)$, and V_s denote for Young modulus, shear modulus, Poisson's ratio, thermal expansion coefficient in fiber direction, thermal expansion coefficient perpendicular to the fiber direction, shear modulus of SMA, and SMA volume fraction, respectively.

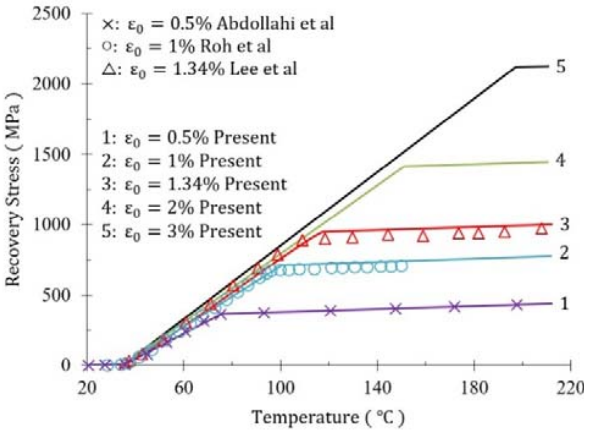

Fig. 3 The SMA wire recovery stress

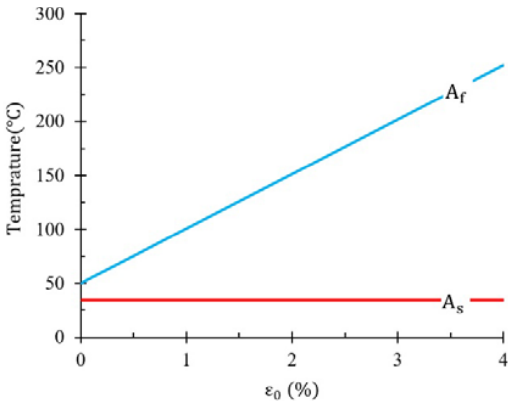

Fig. 4 The effect of SMA pre-strain on the austenite start and finish temperature

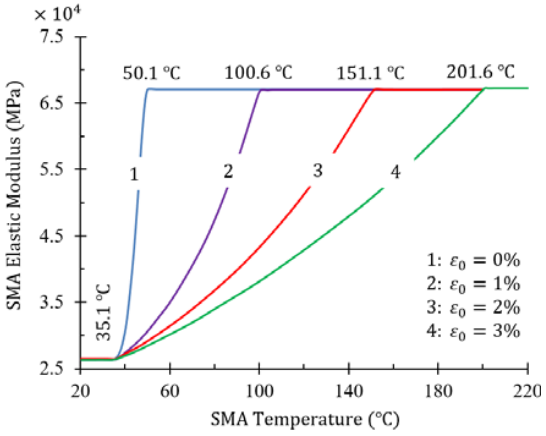

Fig. 5 SMA temperature-dependent elastic modulus

According to the FSDT, the displacement components of a shell are as follows:

$$\begin{bmatrix}\varepsilon_x\\ \varepsilon_y\\ \gamma_{xy}\end{bmatrix}=\begin{bmatrix}\varepsilon_x^0\\ \varepsilon_y^0\\ \gamma_{xy}^0\end{bmatrix}+z\begin{bmatrix}\kappa_x^0\\ \kappa_y^0\\ \kappa_{xy}^0\end{bmatrix}$$
$$\begin{bmatrix}\varepsilon_x^0\\ \varepsilon_y^0\\ \gamma_{xy}^0\end{bmatrix}=\begin{bmatrix}\frac{\partial u_0}{\partial x}+\frac{1}{2}\left(\frac{\partial w_0}{\partial x}\right)^2\\ \frac{\partial v_0}{\partial y}-\frac{w_0}{R}+\frac{1}{2}\left(\frac{\partial w_0}{\partial y}\right)^2\\ \frac{\partial u_0}{\partial y}+\frac{\partial v_0}{\partial y}+\frac{\partial w_0}{\partial x}\frac{\partial w_0}{\partial y}\end{bmatrix}$$
$$\begin{bmatrix}\kappa_x^0\\ \kappa_y^0\\ \kappa_{xy}^0\end{bmatrix}=\begin{bmatrix}\frac{\partial \varphi_x}{\partial x}\\ \frac{\partial \varphi_y}{\partial y}\\ \frac{\partial \varphi_x}{\partial y}+\frac{\partial \varphi_y}{\partial x}\end{bmatrix}$$
$$\begin{bmatrix}\gamma_{xz}\\ \gamma_{yz}\end{bmatrix}=\begin{bmatrix}\varphi_x+\frac{\partial w_0}{\partial x}\\ \varphi_y+\frac{\partial w_0}{\partial y}\end{bmatrix} \quad (12)$$

where ε_x and ε_y are the normal strains, and γ_{xy} is the shear strain. u_0 and v_0 are the shell displacements in the x and y directions, and w_0 is the lateral deflection. φ_x and φ_y are the rotation terms about the y and x axes.

Stress-strain in a laminate reinforced with SMA wires (in global coordinate), is:

$$\begin{bmatrix}\sigma_x\\ \sigma_y\\ \tau_{xy}\end{bmatrix}=\begin{bmatrix}\bar{Q}_{11} & \bar{Q}_{12} & 0\\ \bar{Q}_{12} & \bar{Q}_{22} & 0\\ 0 & 0 & \bar{Q}_{66}\end{bmatrix}\begin{bmatrix}\varepsilon_x\\ \varepsilon_y\\ \gamma_{xy}\end{bmatrix}+V_s\begin{bmatrix}\sigma_x^r\\ \sigma_y^r\\ 0\end{bmatrix} \quad (13)$$

where $\bar{Q}_{ij}$ defines the reduced stiffness matrix and σ^r is the SMA tensile recovery stress.

The stress resultants are defined as:

$$\left(\begin{bmatrix}N_x\\ N_y\\ N_{xy}\end{bmatrix},\begin{bmatrix}M_x\\ M_y\\ M_{xy}\end{bmatrix}\right)=\int_{-\frac{t}{2}}^{\frac{t}{2}}\begin{bmatrix}\sigma_x\\ \sigma_y\\ \tau_{xy}\end{bmatrix}(1,z)dz$$
$$\begin{bmatrix}Q_x\\ Q_y\end{bmatrix}=\int_{-\frac{t}{2}}^{\frac{t}{2}}\begin{bmatrix}\tau_{xz}\\ \tau_{yz}\end{bmatrix}dz \Rightarrow \begin{bmatrix}Q_x\\ Q_y\end{bmatrix}=K\begin{bmatrix}A_{44} & A_{45}\\ A_{45} & A_{55}\end{bmatrix}\begin{bmatrix}\varphi_x+\frac{\partial w_0}{\partial x}\\ \varphi_y+\frac{\partial w_0}{\partial y}\end{bmatrix} \quad (15)$$

The recovery and thermal force resultants are:

$$\begin{bmatrix}N_x^r\\ N_y^r\\ 0\end{bmatrix}=\sum_{p=1}^{N}\int_{t_{p-1}}^{t_p}\begin{bmatrix}\sigma_x^r\\ \sigma_y^r\\ 0\end{bmatrix}V_s dz$$
$$\begin{bmatrix}N_x^T\\ N_y^T\\ 0\end{bmatrix}=\sum_{p=1}^{N}\int_{t_{p-1}}^{t_p}\begin{bmatrix}\bar{Q}_{11}\alpha_x+\bar{Q}_{12}\alpha_y\\ \bar{Q}_{12}\alpha_x+\bar{Q}_{22}\alpha_y\\ 0\end{bmatrix}\Delta T dz \quad (16)$$

where N_x, N_y, N_{xy}, M_x, M_y, M_{xy}, N_x^T, N_y^T, N_x^r and N_y^r are the force resultants, Moment resultants, thermal force resultants and the recovery forces of the SMA, respectively. Also, each ply has the same thickness of t_p. p and N denote for the ply and total number of plies. The shear correction factor $K = 5/6$.

By calculating the mathematical integrations (15) and (16), the relations between stress resultants and strains can be obtained as:

$$\begin{bmatrix}N_{3\times1}\\ M_{3\times1}\end{bmatrix}=\begin{bmatrix}A_{3\times3} & 0\\ 0 & D_{3\times3}\end{bmatrix}\begin{bmatrix}\varepsilon_{3\times3}\\ \kappa_{3\times3}\end{bmatrix}-\begin{bmatrix}N_{3\times3}^T\\ 0\end{bmatrix}+\begin{bmatrix}N_{3\times3}^r\\ 0\end{bmatrix} \quad (17)$$

A_{ij} and D_{ij} are the shell stiffness defined as:

$$(A_{ij}, D_{ij})=\int_{-\frac{t}{2}}^{\frac{t}{2}}\left[\bar{Q}_{ij}\right](1,z^2)dz \quad (i,j=1,2,4,5,6) \quad (18)$$

In the present paper, simply supported at two ends as boundary conditions is considered. The lateral deflection of the shell (w_0) and the rotation functions (φ_x and φ_y) are assumed to be:

$$w_0 = W sin\frac{m\pi x}{L} sin\frac{ny}{R}$$
$$\varphi_x = \Phi_x cos\frac{m\pi x}{L} sin\frac{ny}{R}$$
$$\varphi_y = \Phi_y sin\frac{m\pi x}{L} cos\frac{ny}{R} \quad (19)$$

where m and n are the half-wave numbers. Φ_x and Φ_y are the functions of W that can be fully determined.

A temperature-dependent composite matrix material [24] is used in the modeling of the SMA composite cylindrical shell. Table II provides the graphite epoxy material property.

TABLE II
THERMO-MECHANICAL PROPERTIES OF THE COMPOSITE MATRIX

Mechanical Parameter	Graphite/Epoxy [24].
$E_{1m}\,(GPa)$	$150(1-0.0005\times\Delta T)$
$E_{2m}\,(GPa)$	$9(1-0.0002\times\Delta T)$
$G_{12m}\,(GPa)$	$7.1(1-0.0002\times\Delta T)$
$\alpha_{1m}\,(℃^{-1})$	$1.1\times10^{-6}(1+0.0005\times\Delta T)$
$\alpha_{2m}\,(℃^{-1})$	$25.2\times10^{-6}(1+0.0005\times\Delta T)$
υ_{12m}	0.3

The equilibrium equations of the composite cylindrical shell are:

$$N_{x,x}+N_{xy,y}=0$$
$$N_{xy,x}+N_{y,y}=0$$
$$M_{x,x}+M_{xy,y}-Q_x=0$$
$$M_{y,y}+M_{xy,x}-Q_y=0$$
$$Q_{x,x}+Q_{y,y}+N_x w_{0,xx}+2N_{xy}w_{0,xy}+N_y w_{0,yy}+\frac{N_y}{R}+q=0 \quad (20)$$

where q is the uniform radial load. The Airy stress function F is defined in order to satisfy the first and the second equilibrium equations (20):

$$N_x = F_{,yy}\,, N_y = F_{,xx}\,, N_{xy} = -F_{,xy} \quad (21)$$

The compatibility equation of the cylinder in terms of the strains and the lateral deflection component is as follows:

$$\varepsilon_{x,yy} + \varepsilon_{y,xx} - \gamma_{xy,xy} = {w_{0,xy}}^2 - w_{0,xx}w_{0,yy} - \frac{w_{0,xx}}{R} \qquad (22)$$

The stress function can be determined by using (17), (19), and (22). The load-deflection curves can be obtained by using the Airy stress function and applying Galerkin technique on the last equation in the equilibrium equation (20). These procedures are performed through a MATLAB code. For validating the presented method, some validation studies are conducted and presented in the next section.

IV. Results and Discussions

A. Validation Studies

In this paper, the non-linear load-deflection response of cylindrical composite shells is validated. Figs. 6 and 7 show comparison studies of the mechanical load-deflection response of two isotropic composite cylindrical shells. The results are validated with outcomes reported by Dung and Nga [25]. The material properties and geometry of the structure can be found in the reference work. Excellent agreement between the results is observed.

B. Parametric Studies

Before conducting parametric studies, it is important to show the effect of temperature-dependent (TD) and temperature-independent (TID) matrix material properties on the non-linear load-deflection of a cylindrical shell. Fig. 8 shows the effect of TD and TID matrix material on the load-deflection curves. Therefore, in order to obtain more realistic results, the temperature-dependent matrix material is considered in all of the following parametric studies.

For parametric studies, the non-linear load-deflection curves of the reinforced structure are plotted in the following figures. In all studies, the constant geometry of the cylinder and stacking sequence are:

$$L = 1000\ mm, R = 500\ mm, t = 2\ mm, [0^{SMA}/90]_s.$$

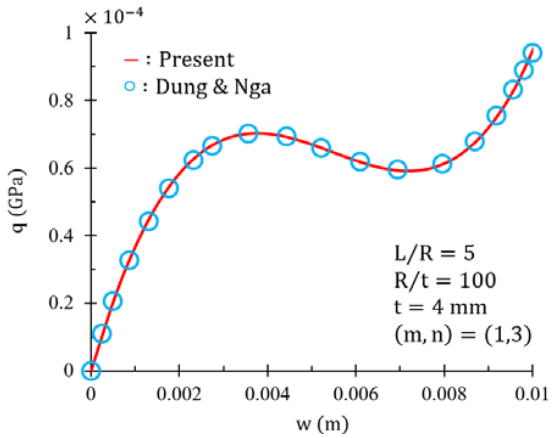

Fig. 6 The first comparison results on the mechanical load-deflection response of laminated composite cylindrical shell

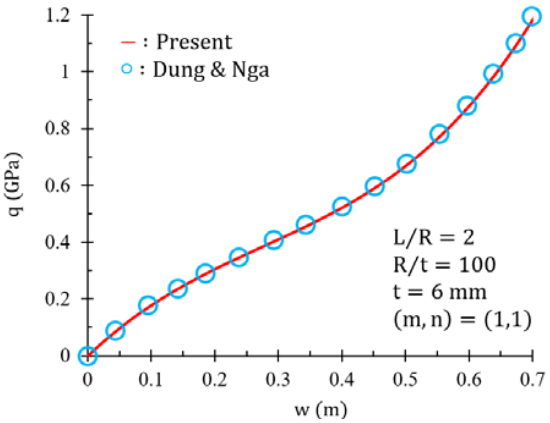

Fig. 7 The second comparison results on the mechanical load-deflection response of laminated composite cylindrical shell

Fig. 9 shows the effect of different SMA volume fractions on the load-deflection response of the cylindrical composite shell. WOS stands for "With-out SMA". As can be seen, an increase in SMA volume fraction leads to higher load-bearing capacity. Similar results on the behavior enhancement of SMA composite structures due to the tensile recovery force of the SMA wires have been shown in Tavousi Tehrani and Kabir's recent works [18], [26].

Fig. 10 demonstrates the effect of different SMA pre-stain values on the response of a composite cylindrical shell. Generally, higher pre-strain values result in higher tensile recovery force, which means higher load-bearing capacity. According to Fig. 3, at activation temperature between austenite start and finish temperatures, the tensile recovery force remains almost constant. Therefore, the curves number 4 and 5 in Fig. 10 are almost coincident. The improvement between WOS cylindrical shell and the SMA-reinforced cylindrical shell is obvious.

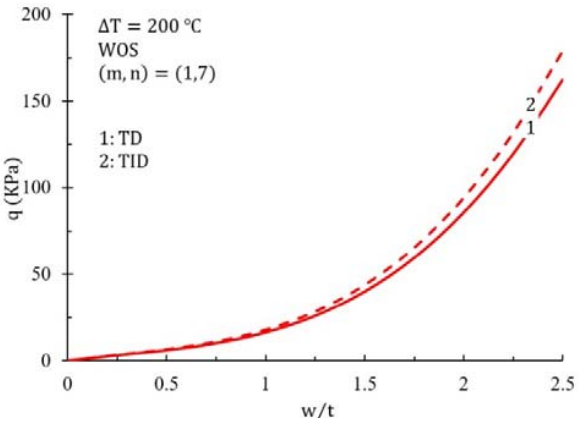

Fig. 8 The effect of TD and TID matrix material properties on the load-deflection response of the laminated composite cylindrical shell

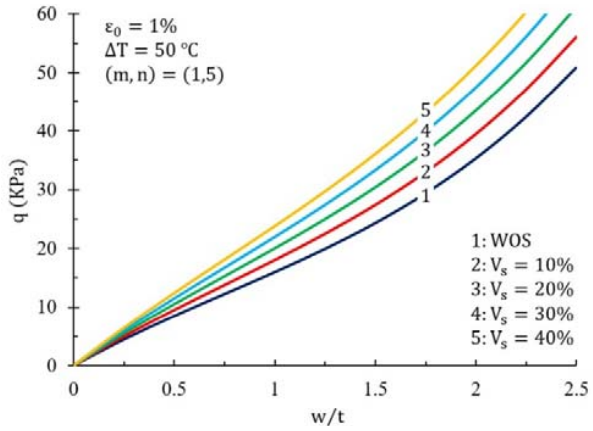

Fig. 9 The effect of different SMA volume fractions on the load-deflection response of the cylindrical shell

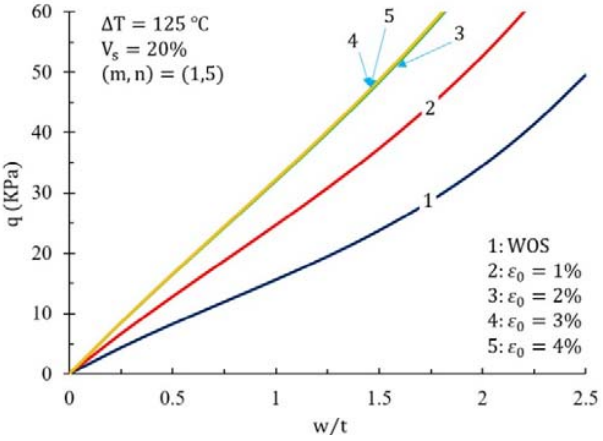

Fig. 10 The effect of different SMA pre-strain values on the load-deflection response of the cylindrical shell

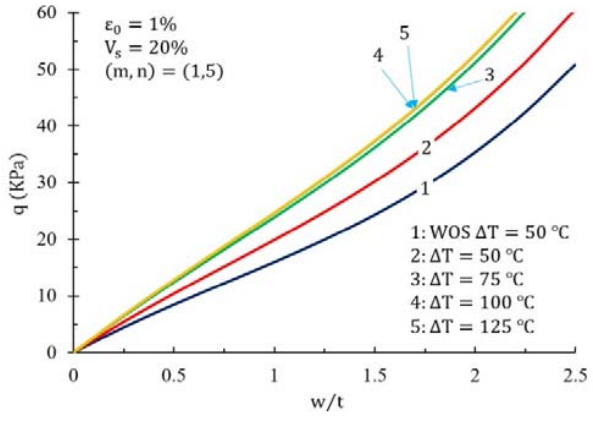

Fig. 11 The effect of different SMA activation temperatures on the load-deflection response of the cylindrical shell

Fig. 11 illustrates the influence of different activation temperatures on the load-deflection response of a composite cylindrical shell. It is obvious that higher activation temperature leads to higher tensile recovery force. According to Fig. 3, once the phase transformation completes, there is no considerable additional recovery force. Therefore, the curves number 4 and 5 in Fig. 11 are almost coincident. The phase transformation finishes at $T = 100.5$ ℃ ($\Delta T = 100.5 - 20 = 80.5$ ℃), as a result, for activation temperatures above $\Delta T = 80.5$ ℃, there is no considerable additional tensile recovery force to enhance the load-deflection response.

V. Conclusions

Circular laminated composite cylindrical shells are widely implemented in structural designs. When these types of structures are subjected to mechanical or thermal loading, their load-bearing capacity is important in the design procedure. In this study, nonlinear equilibrium equations for simply supported SMA composite cylindrical shell under uniform radial load are solved. The effects of different SMA volume fractions, SMA pre-strain values, and activation temperatures on the response of the structure are investigated. It is concluded that:

- The shells with higher SMA volume fractions can withstand a higher uniform radial load.
- Higher activation temperature leads to higher load-bearing ability for the structure. The activation temperatures should be below the austenite finish temperature to obtain suitable results.
- Higher pre-strain values result in a better load-deflection response. At temperatures between austenite start and finish temperatures, the tensile recovery force remains almost constant.
- Generally, the presence of SMA wires results in a decrease in the structure's lateral deflection in comparison with the WOS shells.

Acknowledgment

The authors would like to thank Eng. Fateme Sabet for her assistance by providing a 3D model of the structure.

References

[1] J. S. N. Paine, C. A. Rogers, and R. A. Smith, "Adaptive Composite Materials with Shape Memory Alloy Actuators for Cylinders and Pressure Vessels," *Journal of Intelligent Material Systems and Structures*, vol. 6, no. 2, pp. 210–219, Mar. 1995.

[2] R. Burgueño, N. Hu, and N. Lajnef, "Controlling the postbuckling response of cylindrical shells under axial compression for applications in smart structures," *ASME 2013 Conference on Smart Materials, Adaptive Structures and Intelligent Systems, SMASIS 2013*, vol. 2, no. July, 2013.

[3] A. R. Damanpack, W. H. Liao, M. M. Aghdam, M. Shakeri, and M. Bodaghi, "Micro-macro thermo-mechanical analysis of axisymmetric shape memory alloy composite cylinders," *Composite Structures*, vol. 131, no. July 2016, pp. 1001–1016, 2015.

[4] S. Nemat-Nasser, J. Yong Choi, J. B. Isaacs, and D. W. Lischer, "Quasi-Static and Dynamic Buckling of Thin Cylindrical Shape-Memory Shells," *Journal of Applied Mechanics*, vol. 73, no. 5, p. 825, 2006.

[5] L. G. Sil'chenko, A. A. Movchan, and T. L. Sil'chenko, "Stability of a cylindrical shell made of a shape-memory alloy," *International Applied Mechanics*, vol. 50, no. 2, pp. 171–178, 2014.

[6] V. Birman, "Theory and comparison of the effect of composite and shape memory alloy stiffeners on stability of composite shells and plates," *International Journal of Mechanical Sciences*, vol. 39, no. 10, pp. 1139–1149, 1997.

[7] H. Asadi, Y. Kiani, M. Aghdam, and M. Shakeri, "Enhanced thermal buckling of laminated composite cylindrical shells with shape memory alloy," *Journal of Composite Materials*, vol. 50, no. 2, pp. 243–256,

2016.
[8] H. Asadi, A. H. Akbarzadeh, Z. T. Chen, and M. M. Aghdam, "Enhanced thermal stability of functionally graded sandwich cylindrical shells by shape memory alloys," *Smart Materials and Structures*, vol. 24, no. 4, p. 045022, 2015.
[9] M. R. Amini and S. Nemat-Nasser, "Dynamic buckling and recovery of thin cylindrical shape memory shells," *Proceedings of SPIE - The International Society for Optical Engineering*, vol. 5761, pp. 450–453, 2005.
[10] T. Akbari and S. M. R. Khalili, "Experimental investigations on the mechanical properties and buckling behavior of the filament wound composite shells embedded with shape memory alloy wires," *Mechanics of Advanced Materials and Structures*, vol. 0, no. 0, pp. 1–7, 2018.
[11] B. Liu and C. Du, "Effects of external pressure on phase transformation of shape memory alloy cylinder," *International Journal of Mechanical Sciences*, vol. 88, pp. 8–16, Nov. 2014.
[12] H. Li, H. Li, and H. Tzou, "Frequency Control of Beams and Cylindrical Shells With Light-Activated Shape Memory Polymers," *Journal of Vibration and Acoustics*, vol. 137, no. 1, p. 011010, Feb. 2015.
[13] F. Forouzesh and A. A. Jafari, "Radial vibration analysis of pseudoelastic shape memory alloy thin cylindrical shells by the differential quadrature method," *Thin-Walled Structures*, vol. 93, pp. 158–168, Aug. 2015.
[14] M. Salim, M. Bodaghi, S. Kamarian, and M. Shakeri, "Free vibration analysis and design optimization of SMA/Graphite/Epoxy composite shells in thermal environments," *Latin American Journal of Solids and Structures*, vol. 15, no. 1, Apr. 2018.
[15] F. Auricchio and E. Sacco, "A one-dimensional model for superelastic shape-memory alloys with different elastic properties between austenite and martensite," *International Journal of Non-Linear Mechanics*, vol. 32, no. 6, pp. 1101–1114, 1997.
[16] L. C. Brinson and M. S. Huang, "Simplifications and Comparisons of Shape Memory Alloy Constitutive Models," *Journal of Intelligent Material Systems and Structures*, vol. 7, no. 1, pp. 108–114, Jan. 1996.
[17] L. C. Brinson, "One-Dimensional Constitutive Behavior of Shape Memory Alloys: Thermomechanical Derivation with Non-Constant Material Functions and Redefined Martensite Internal Variable," *Journal of Intelligent Material Systems and Structures*, vol. 4, no. April, pp. 229–242, 1993.
[18] M.-Z. Kabir and B. Tavousi Tehrani, "Closed-form solution for thermal, mechanical, and thermo-mechanical buckling and post-buckling of SMA composite plates," *Composite Structures*, vol. 168, pp. 535–548, May 2017.
[19] C. Liang, "The Constitutive Modeling of Shape Memory Alloys," Virginia Polytechnic Institute and State University, 1990.
[20] H. J. Lee, J. J. Lee, and J. S. Huh, "A simulation study on the thermal buckling behavior of laminated composite shells with embedded shape memory alloy (SMA) wires," *Composite Structures*, vol. 47, no. 1, pp. 463–469, 1999.
[21] J.-H. Roh, I.-K. Oh, S.-M. Yang, J.-H. Han, and I. Lee, "Thermal post-buckling analysis of shape memory alloy hybrid composite shell panels," *Smart Materials and Structures*, vol. 13, no. 6, pp. 1337–1344, 2004.
[22] H. Abdollahi, S. E. Esfahani, M. Shakeri, and M. R. Eslami, "Non-Linear Thermal Stability Analysis of SMA Wire-Embedded Hybrid Laminated Composite Timoshenko Beams on Non-Linear Hardening Elastic Foundation," *Journal of Thermal Stresses*, vol. 38, no. 3, pp. 277–308, Feb. 2015.
[23] C. C. Chamis, "Simplified Composite Micromechanics Equations of Hygral, Thermal, and Mechanical Properties," in *Thirty-eighth Annual Conference of the Society of the Plastics Industry (SPI) Reinforced Plastics/Composites Institute*, 1983.
[24] M. Bohlooly and B. Mirzavand, "Closed form solutions for buckling and postbuckling analysis of imperfect laminated composite plates with piezoelectric actuators," *Composites Part B: Engineering*, vol. 72, no. 0, pp. 21–29, 2015.
[25] D. Van Dung and N. T. Nga, "Nonlinear buckling and post-buckling of eccentrically stiffened functionally graded cylindrical shells surrounded by an elastic medium based on the first order shear deformation theory," *Vietnam Journal of Mechanics*, vol. 35, no. 4, pp. 285–298, Nov. 2013.
[26] B. Tavousi Tehrani and M.-Z. Kabir, "Non-linear load-deflection response of SMA composite plate resting on winkler-pasternak type elastic foundation under various mechanical and thermal loading," *Thin-Walled Structures*, vol. 129, no. C, pp. 391–403, Aug. 2018.